ARCHITECTURE AND FIRST ACHIEVEMENTS OF A SIMULATION FOR THE APPROACH OF AN UNCOOPERATIVE TARGET

S. Peters[1], W. Eidel[1], R. Förstner[1], and H. Fiedler[2]

[1]*Institute of Space Technology & Space Applications, Universität der Bundeswehr München, DE 85577 Neubiberg, Email: {susanne.peters, werner.eidel, roger.foerstner}@unibw.de*
[2]*German Space Operations Center (GSOC), DLR Oberpfaffenhofen, DE 82234 Weßling, Email: Hauke.Fiedler@dlr.de*

ABSTRACT

With space debris becoming more and more a concern for satellite operators, efforts need to be initiated to sustain a safe space environment and stop the permanent increase of debris. One of many is the active removal of large objects - 5 to 15 per year. The present paper introduces a concept based on a kit-chaser system: A chaser satellite will attach kits to multiple targets. The kit-target set-up will de-orbit controlled, while the chaser proceeds with capturing targets to equip them with a kit.

For testing purposes, a simulation is derived for this concept. The paper presents the multiple modules the simulation is build on. The approach starts at a distance of about 11 m in close vicinity. The method of capture is a robotic arm.
Future developments can focus on various modules to be added and/or existing ones to be adjusted to further requirements or specifications. The implementation of self-awareness for the chaser to react to unexpected situations or failures without the need for a signal from the ground-station.

Keywords: uncooperative target, simulation, approach.

1. SPACE DEBRIS

In the past decades, space debris has become a growing concern for satellite operators. To sustain the current environment around Earth, mitigation measurements such as an improved observation or implementation of post-mission disposal have taken place and are further developed. Regarding long-term sustainability, a repeated active debris removal of 5 to 15 large objects per year - objects that have a mass of at least one ton - has to be included to stabilize the orbits. An otherwise starting cascade effect would prohibit the use of the affected orbits and with that limit missions in space.

While the prediction for debris trajectories and maneuver, how to avoid them, have improved, still about 3 collision avoidance maneuvers (CAM) per satellite and year have to be performed. CAM can only be performed in case of a warning. If the approaching object however was not tracked - for example due to its size - no command will be given and a collision may decommission the satellite. Another feared scenario is the collision of two large objects that both cannot maneuver. An incident of two rocket bodies of the SL-16 type, for example, could double the number of the known debris in low Earth orbit (LEO). They have been observed to have missed each other by a few milli-arc-seconds [1]. Especially with the latter scenario in mind, the active removal of debris is inevitable.

Additional mitigation measurements are already implemented. These measurements include post-mission disposal, limiting of mission-related debris, limiting of potential explosions by e.g., releasing left-over propellant, limiting the probability of accidental collisions or avoiding an intentional destruction and other harmful activities [2]. However, even when successfully implementing those measurements, an increase in the number of debris objects is conceivable from the simulations. Only the constant removal of 5 to 15 large objects of highly frequented orbits per year will have an influence on the long term stabilization of the LEO space environment [3].

The approach presented within this paper addresses the removal of at least 5 large objects to be removed controlled within one year. With rendezvous and docking with an uncooperative object never having been performed, a wide range of challenges have to be met. The object of choice will not send any data on its altitude or motion, it will not have a pre-designed point of contact for e.g., grabbing, and there will be no way of communication with it. Close vicinity may lead to the point where a command from a ground station could be sent too late, with the possible result of a collision of the two objects.

Having those considerations in mind, the *A*utonomous *D*ebris *R*emoval *Sa*tellite - #A (ADReS-A) is conceptualized. ADReS-A targets multiple SL-8 rocket bodies to provide them with a de-orbit kit for controlled reentry. The concept aims to improve the self-awareness of a chaser satellite with the ability to react to failures while in close vicinity. Sufficient testing is required as the influence on objects in space is limited. Thus, a sim-

Proc. 7th European Conference on Space Debris, Darmstadt, Germany, 18–21 April 2017, published by the ESA Space Debris Office
Ed. T. Flohrer & F. Schmitz, (http://spacedebris2017.sdo.esoc.esa.int, June 2017)

ulation based on the demands of ADReS-A shall support the concept. As the simulation is derived from the mission concept, an introduction to the concept of ADReS-A is given at first.

2. MISSION CONCEPT

The idea behind ADReS-A was presented in much more detail in previous work, and can be found for example in Reference [4] or [5]. A summary of the concept is given in the following.

2.1. Mission Architecture

As mentioned in Section 1, large objects are targeted. ADR has to be performed for many years and should therefore be as effective and efficient as possible. It will hardly be cost wise favorable to launch only one removal chaser per mission. Hence, ADReS-A consists of a main chaser and multiple de-orbit kits. While the chaser - ADReS-A - incorporates most of the complexity regarding docking and maneuvering techniques, the kits are designed simpler. They will de-orbit together with the target and be lost during the reentry. Their task is to perform the de-orbit in a controlled way to an uninhabited area. ADReS-A needs the maximum of flexibility and will therefore carry one kit at a time to the designated target, while the other kits wait in a parking orbit somewhat lower than the target's orbit. Other concepts to be found in the literature concentrate mainly on the removal of one object or the technology behind it, rather than addressing the whole problem of long-term sustainability of the space environment. The simulation derived follows this example, but is based on a concept for multiple removal. Figure 1 gives a preliminary mission time line of the concept.

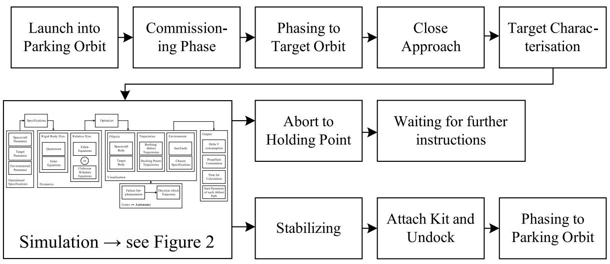

Figure 1. Mission time line for ADReS-A. The simulation covers the part from close approach (< 11 m) and mating.

2.2. Target

Efficiency is one of the main goals of ADReS-A. A study performed in 2013 by the author analyzed the available data of about 17.000 objects of the SatCat [6] according to collision probability and hazardousness of such. As predicted, large objects were the most influential objects. Further on, the study analyzed those objects according to their vicinity - taking into consideration that one chaser has to travel between multiple objects while consuming as little propellant as possible. SL-8 rocket bodies (SL-8 R/Bs) turned out to gather in at least three different orbits - two around 74 degrees inclination at an altitude of 1500 to 1600 km and 700 to 800 km, respectively, and one at an inclination of about 82 degrees at an altitude of 900 to 1000 km. No other objects of a similar type were found to be as close to each other as the SL-8 R/Bs. Hence, the orbit concentrating most of the rocket bodies (the latter one), was chosen as mission orbit with SL-8 R/Bs as targets.

2.3. Satellite Design

Based on the target selection and the mission architecture, a chaser satellite (ADReS-A) and de-orbit kits are designed. For removal technology, a robotic arm resulted from a weighing analysis that covered heritage, complexity, re-usability, and similar aspects. The largest advantage of a robotic arm is its legacy and possible use for on-orbit servicing, a promising field of business development in space which again makes financing of such mission more likely.
The chaser has a second, linear, arm to carry and attach the de-orbit kit. The kit will be attached to the target's nozzle, using a clamp mechanism for a stable connection. The nozzles physical parameters promise the most robust connection. The satellite design can be found in more detail in Reference [5].

3. SIMULATION

When developing a simulation, certain considerations have to be taken into account. What shall be shown by the simulation? What modules have to be included to reach that goal? Which functionalities shall form the basis of the simulation? Which level of detail is meant to be provided by the simulation? What simplifications compared to reality are acceptable? etc. The following section reasons the decisions made for the simulation regarding the approach of ADReS-A. After the frame is presented, the multiple modules included and displayed in Figure 2 are presented. The level of detail and simplifications accepted are explained within their description.

3.1. Frame for simulation

The motivation for creating a simulation for the docking process derives from the need to test various strategies before realizing such a mission. Active debris removal has never been performed in space. Ideas on what challenges to overcome and which difficult events may occur can be derived from missions that cover the very close

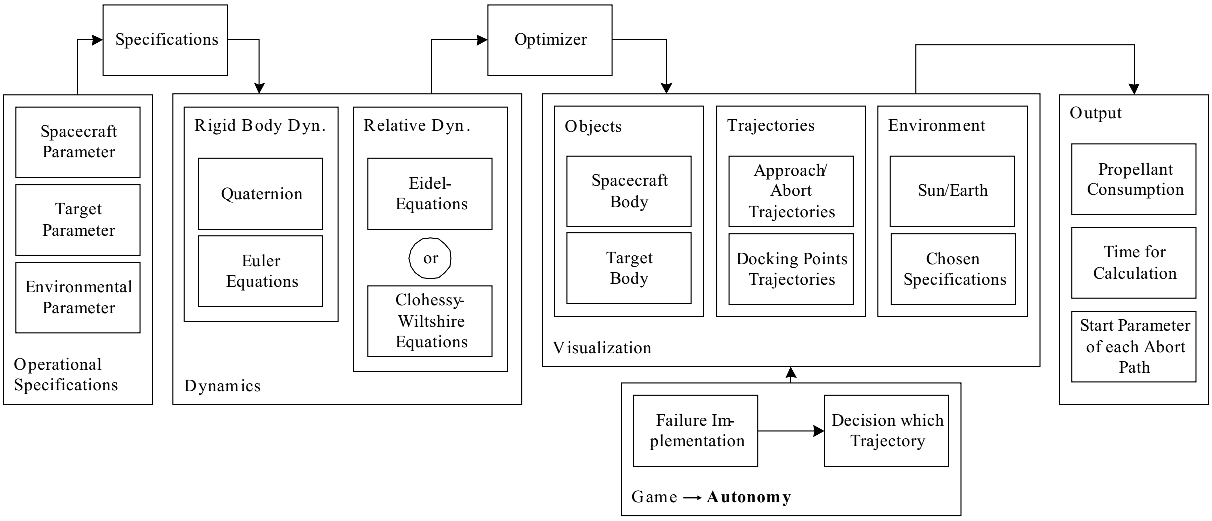

Figure 2. Architecture for the Simulation of ADReS-A

approach or rendezvous procedures. Docking has been performed manually on the International Space Station, and some behaviors may be derived from there. However, an uncooperative target never designed to be handled in space will bring up various occurrences that cannot be foreseen. A simulation may help to understand and thus prepare for some of them. The simulation of ADReS-A is built from modules, as can be seen in Figure 2. This object-oriented programming allows us to vary parameters without changing the whole process, and to add and delete modules. These features will be of advantage once the simulation is further developed.

As shown in Figure 1, the simulation of ADReS-A will cover the part of the close approach once in reach of 11 m distance along the direction of flight up to the actual rendezvous & docking of the two systems. At this distance, the camera in use is able to track the detailed motion of the target, needed for a a safe approach [7]. Calculated are the approach to a moving docking point and multiple abort trajectories in case of a failure or contradictory data that cannot be solved.
The level of detail is quite low at this point of the development. However, due to the modular-setup, changes can be implemented if necessary or required.

3.2. Operational Specifications

The simulation requires the input of at least 43 parameters. 6 of them cover the satellite's and target's relative position (x,y,z-direction), 6 cover their relative velocity (v_x, v_y, v_z) and an additional 6 give statements about the objects angular velocity ($w_{Sx}, w_{Sy}, w_{Sz}; w_{Tx}, w_{Ty}, w_{Tz}$). 6 more address the objects orientation (given in quaternions), 3 parameters describe each objects dimension (2 x radius, 4 x length from each center of mass forward and backward). Moreover, the inertia torques have to be assigned (3 parameters each). For now, two parameters define possible optimization implementations. The available maximal thrust, momentum and allowed time for the trajectory have to be assigned, as well the position of the docking points. Additional information can be adapted concerning any weighing of the optimization parameters, a safety area to avoid a collision at any time, or any area limitations the chaser is not allowed to enter when approaching the target.

3.2.1. Environmental Parameter

In accordance with Section 2.2, an orbit of 970 km altitude with an inclination of 82.9 degrees is aimed for. The parking orbit will be about 30 km below the target's orbit. An analysis performed concerning the radiation and electrostatic charges [8] revealed a usual exposure. Especially with the mission lasting one year, no extraordinary precaution is planned.
The simulation is based on the relative dynamics of the two systems (target & chaser+kit). As the two objects are really close and and show similar mass and size, perturbations will act very similar to them. Therefore, no perturbations such as the J2-term, the gravity-gradient, solar radiation pressure, Earth's magnetic field or the objects aerodynamic drag are considered.

3.2.2. Target Parameter

As mentioned in Section 2.2, SL-8 R/Bs are targeted. The simulation needs input about their size, mass and inertia torque which are derived from the CAD-design.
With the rocket bodies being of Soviet Union origin, actual CAD-data is hard to find. The design shown in Figure 3 is based on References [9] and [10]. Another vague data is their mass. Their dry mass is known to be about 1.4 t. However, they did not deflate unused propellant as

is proposed nowadays. An additional weight of 200 kg (about 14%) was thus added for the calculations. Especially with left-over propellant, the chance for sloshing is high, however, the rocket bodies inertia torque was derived from an assumed homogenous distribution of the mass.

3.2.3. Spacecraft & Kit Parameter

With the spacecraft and de-orbit-kit CAD-design, the data about mass, size and inertia torque are extracted. Sloshing will not be considered at this point. The satellites mass is about 1.1 t (wet), the mass of one kit is about 500 kg (wet). The kit will be carried inside the body of ADReS-A. Figure 3 shows the object's CAD models. A simplification for the simulation transfers the models into a cylindrical shape.

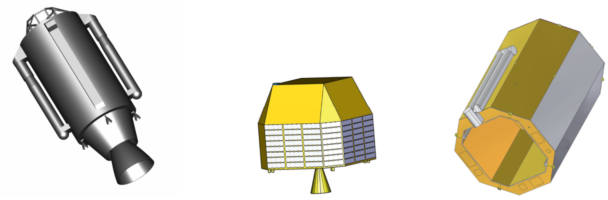

Figure 3. Involved objects for the mission (not scaled). **Left***: SL-8 R/B;* **Middle***: Kit;* **Right***: ADReS-A*

3.3. Specifications

Operational specifications address the special needs of the mission during the approach. One specification, which is not part of the simulation but needs to be considered beforehand, is the illumination of the target by the sun. To calculate the correct motion rate, the camera needs about 130 min [7]. However, it does not work adequate by shadow or darkness, neither when facing the Sun directly nor when her reflection on the surface of the target is too bright. Thus, the time of one orbit revolution of about 90 min is limited to nearly 52 min observation time. The proof of fully charged batteries for a maximum in operation time, enough propellant or antenna pointing are other specifications that need to be handled outside the simulation.
Operational specifications that influence the simulation directly are, for example, the exact time when a maneuver can take place so sensitive sensors are not harmed by light or shadow. The battery status will need to be supervised as well as the functionality of the subsystems.

3.4. Dynamics

While the whole mission requires absolute and relative navigation, the simulation is based on relative dynamics and rigid body dynamics.

3.4.1. Coordinate Systems

To describe the motion of the two (three) involved objects, multiple coordinate systems are in use. The local-vertical, local-horizontal (LVLH) system, cf. Alfriend [12], describes the relative position of the objects. Tow additional coordinate systems are body-fixed and centered in the target and spacecraft&kit models. The coordinate systems are required to describe the the objects orientation in space. The quaternions in use solve the problem of singularity of the also commonly used Euler angles. The implementation of the Euler Equations allow for the two docking points - one belonging to ADReS-A, the other to the SL-8 R/ - to rotate within the simulation and describe the rigid body dynamics. In an unrotated state, the axis of the body-fixed system align with the ones used in the LVLH-system.

3.4.2. Relative Dynamics

Relative dynamic calculations can be adequately used for any distance smaller than 100 m. As the simulation aims to provide a tool for the analysis and verification of different strategies, it is obvious to use rather analytic equations for the approach than numerical. The Hill's equations or Clohessy-Wiltshire (CW) equations provide a suitable approximation for the numerical approach, derived for near-circular orbits. The SL-8 R/Bs orbits have an eccentricity of about 0.003, the use of CW-equations is thus considered suitable. The following figures give an idea about their accuracy if adapted to the discussed ADR-mission.
For the simulation of ADReS-A, efforts for a more precise analytic approach were made. The Eidel-equations are derived for small elliptical orbits with eccentricities smaller than 0.1. They add an additional term to the CW-equations, as can be seen in Equations 1 to 3. In consistence, they use the LVLH-coordinate system with the origin of ordinates within the satellite. In contrast, the axes are pointing in different directions - η is parallel to the vector of the angular momentum (similar to the z-axis in the CW-equations), ζ is defined as the extension of the connection of the center of Earth to the satellite pointing out of orbit (like the x-axis in the CW-equations) and ξ completes the orthogonal tripod (while the corresponding y-axis in the CW-equations points into the direction of flight).

Complete system of equations according to Eidel [11]

$$\xi_{Eid} = \xi^{(0)} + e\xi^{(1)} \tag{1}$$

$$\eta_{Eid} = \eta^{(0)} + e\eta^{(1)} \tag{2}$$

$$\zeta_{Eid} = \zeta^{(0)} + e\zeta^{(1)} \tag{3}$$

The first part reflects the CW-equations:

$$\xi^{(0)} = 2\zeta_0' \cos\tau + (6\zeta_0 + 4\xi_0')\sin\tau - 3(\xi_0' + 2\zeta_0)\tau + \xi_0 - 2\zeta_0' \tag{4}$$

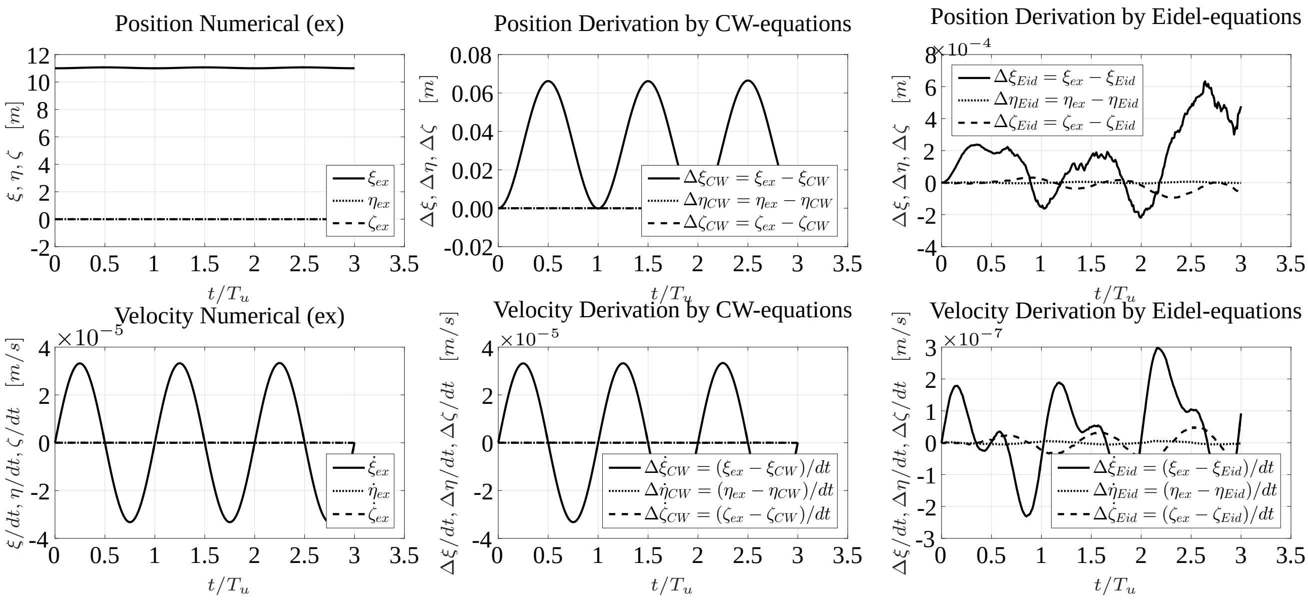

Figure 4. Exact position and velocity of the two systems with no relative velocity and a 11 m distance in the direction of flight. Derivation resulting by using the analytic approach of Clohessy-Wiltshire and Eidel are given in the middle and right hand graphics. The x-axis counts the orbits taken.

$$\eta^{(0)} = \eta_0 \cos\tau + \eta_0' \sin\tau \tag{5}$$

$$\zeta^{(0)} = -(3\zeta_0 + 2\xi_0')\cos\tau + \zeta_0'\sin\tau + 2(2\zeta_0 + \xi_0') \tag{6}$$

and the second part defines the relative dynamics more precisely:

$$\begin{aligned}\xi^{(1)} = {} & 4[(5\zeta_0 + \xi_0')\cos\theta_0 - (\xi_0 - 2\zeta_0')\sin\theta_0]\sin\tau \\ & - 2[2\zeta_0'\cos\theta_0 + \xi_0'\sin\theta_0]\cos\tau \\ & + \frac{3}{2}(3\zeta_0 + 2\xi_0')\sin(2\tau + \theta_0) + \frac{3}{2}\zeta_0'\cos(2\tau + \theta_0) \\ & + 3(2\zeta_0 + \xi_0')[\sin(\tau + \theta_0) - \tau\cos(\tau + \theta_0)] \\ & - 7(2\zeta_0 + \xi_0')\sin(\tau + \theta_0) - (\xi_0 - 2\zeta_0')\cos(\tau + \theta_0) \\ & - 3[(5\zeta_0 + \xi_0')\cos\theta_0 - (\xi_0 - \zeta_0')\sin\theta_0]\tau \\ & + (3\xi_0' + \frac{7}{2}\zeta_0)\sin\theta_0 + (\xi_0 + \frac{1}{2}\zeta_0')\cos\theta_0 \end{aligned} \tag{7}$$

$$\begin{aligned}\eta^{(1)} = {} & (\eta_0\cos\theta_0 - 2\eta_0'\sin\theta_0)\cos\tau \\ & + (\eta_0\sin\theta_0 - \eta_0'\cos\theta_0)\sin\tau \\ & + \frac{1}{2}\eta_0[\cos(2\tau + \theta_0) - 3\cos\theta_0] \\ & + \frac{1}{2}\eta_0'[\sin(2\tau + \theta_0) + 3\sin\theta_0] \end{aligned} \tag{8}$$

$$\begin{aligned}\zeta^{(1)} = {} & -2[(5\zeta_0 + \xi_0')\cos\theta_0 - (\xi_0 - 2\zeta_0')\sin\theta_0]\cos\tau \\ & - [2\zeta_0'\cos\theta_0 + \xi_0'\sin\theta_0]\sin\tau \\ & - (3\zeta_0 + 2\xi_0')\cos(2\tau + \theta_0) + \zeta_0'\sin(2\tau + \theta_0) \\ & - 3(2\zeta_0 + \xi_0')\tau\sin(\tau + \theta_0) + (13\zeta_0 + 4\xi_0')\cos\theta_0 \\ & + (3\zeta_0' - 2\xi_0)\sin\theta_0. \end{aligned} \tag{9}$$

In Equations 4 to 9, τ is the nominated time variable $\omega_0 \cdot t$ with

$$\omega_0 = \sqrt{\frac{\mu}{(a(1-e^2))^3}}. \tag{10}$$

Here, μ is the gravitational parameter, a the semi-major axis and e the eccentricity of the orbit. θ_0 in Equation 7 to 9 represents the true anomaly at the time $t = 0$. The initial conditions are given by $\xi(0) = \xi_0; \eta(0) = \eta_0; \zeta(0) = \zeta_0; \xi'(0) = \xi_0'; \eta'(0) = \eta_0'$ and $\zeta'(0) = \zeta_0'$. The whole derivation was performed by Dr. Eidel [11].

To get a better understanding of how much influence the Eidel-equations have on the accuracy of the simulation, the following figures compare the numerical calculations with the CW-equations and the Eidel-equations.

In Figure 4 and Figure 5, the accuracy of the different approaches compared to each other is displayed. A higher dependency of the different variables can be derived for the Eidel-equations. Additionally, the Eidel-equations show a 100x higher precision for the position and velocity derivation after 3 orbits in both cases e.g., in case no relative velocity is involved and a relative velocity of 0.01 m/s in every direction at the same distance is assumed.

For now, the CW-equations are applied to the simulation as they are much simpler and deviate from the numerical calculations by only 0.6%. With all the simplifications implemented at the moment, the high precision calculations by Eidel would not make much of a difference. Once a higher accuracy is required, they will be a very good choice to be implemented for a better analytic analysis.

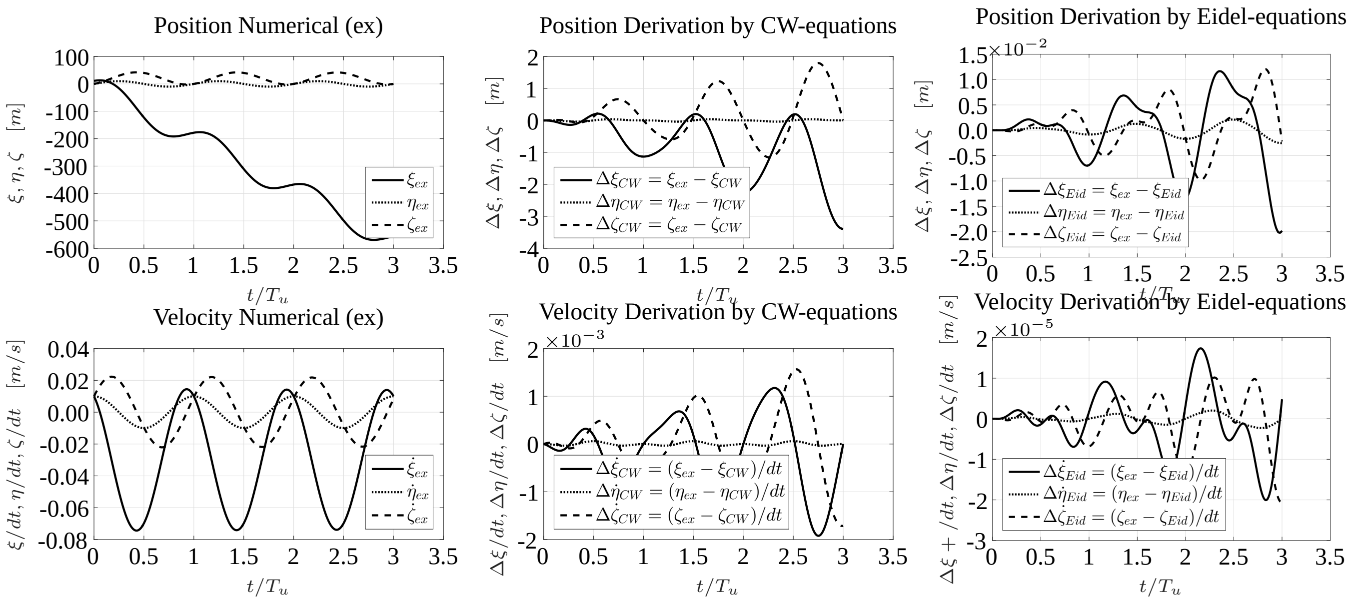

Figure 5. Exact position and velocity of the two systems with a relative velocity of 0.01 m/s in every direction and a 11 m distance in the direction of flight. Derivation resulting by using the analytic approach of Clohessy-Wiltshire and Eidel are given in the middle and right hand graphics. The x-axis counts the orbits taken.

3.5. Optimizer

For the optimal path planning, the work of Michael et al. [13] was applied. The addressed optimization problem in his work was solved using the software package OCPID-DAE1, cf. Gerdts [14]. Here, a robust sequential quadratic programming (SQP) method is combined with a gradient calculation using sensitive implicit differential equations (DAE)s. The package "is suitable for optimal control problems subject to differential algebraic equations of index one" [13].
While the package allows for the optimization of more than one subject, the presented work focuses on a minimum energy consumption. This allows for a cost limitation as the required energy is directly proportional to the propellant and thus to weight and costs of the mission. Other subjects of optimization could be time or a combination of the two. Further work will analyze the mission accordingly. As displayed in Figure 2, the required input is a combination of the mission parameters and the relative dynamics. The output of the optimizer is the approach trajectory, which is then further processed for failure implementation.

3.6. Visualization

3.6.1. Objects

The involved objects are modeled and exists as 3D CAD versions as shown in Section 3.2.3. For a faster calculation, they are simplified as cylinders. The spacecraft and kit together form a cylinder of 2.35 m in diameter and 3 m in length. A rocket body cylinder has a length of 6.6 m and a diameter of 2.4 m. The detailed design can be implemented for visualization or more detailed calculations if required. The mass and initial torque of the CAD model is mirrored as designed.

3.6.2. Berthing

The design of ADReS-A includes a robotic arm. Time for the grabbing maneuver and thus final attachment has to be provided after the chaser has reached its intended position. A berthing box not exceeding the arm's limitations shall give the required flexibility for the final attach. As seen from Section 3.4.2, drift will affect the two objects, attitude control will be required to limit the effect. During the grabbing, however, such action may be harmful. The box gives an area, in which the chaser can drift without the attitude control adjusting. Time limitations for the final docking can be derived using the equations presented. The simulation ends with the two docking points mating. It has to be mentioned that the mating point presents two points within the berthing box with the final approach performed by the robotic arm - a maneuver out of the scope of this work.

3.6.3. Trajectories

The approach trajectory is derived from the formerly listed modules. It describes the trajectory most propellant-saving and ends with the two docking points mating. Any considerations about the stabilization of a potentially tumbling target is not part of the simulation and therefore not part of the discussion. Data derived from the simulations give information about the relative distance, relative velocity and required thrust for the time of the approach.

The abort trajectory is calculated with the same equations used for the approach trajectory. As a result, depending on the number of abort trajectories chosen and the safety parameter implemented, the time for calculation is multiplied (for a direct approach 685 s of processing time is required). Hence, those trajectories need to be calculated beforehand to react in time as the total approach will take about 8 min. Once the whole approach has been initiated and a failure occurs during the maneuver, the spacecraft will choose from its memory the abort trajectory next to come. It will not take the closest trajectory, as this might be the one just passed and a turn around is simply not realistic.

3.6.4. Environment

The visualization of the environment mirror the parameter included. Sun and Earth pose possible perturbations, and are thus displayed.

3.7. Game → Autonomy

When considering the active removal of an object never designed for such, events of unforeseen failures or misleading sensor-data will occur more often than during established spacecraft missions. The proven handling in case of a failure is the switch into safe-mode, with the spacecraft expecting further instruction from ground. For ADR, the approaching spacecraft has no time to wait for a ground-station recover signal as the very close vicinity and possible drift may result in a collision. Hence, onboard processing, fault management and self-awareness of the spacecraft are the key technologies that need to be pushed forward. One step towards that is the on-going development of on-board processor capabilities. Even though a few years behind Earth's PC-development, the progress looks promising [15].

3.7.1. Failure Implementation

For now, the autonomy should rather be called automation and is limited to deciding, which abort trajectory has to be taken after a failure occurs during the approach. The request is to take the next abort trajectory in line, aiming to react as soon and as efficient as possible, as propellant is one of the restricted resources on board a spacecraft. Failures are implemented randomly for now and are addressed further in Section 4.

3.8. Output

Figure 6 gives an idea of the graphical representation of the trajectories that could be followed. The origin of ordinates is positioned within the target (LVLH-system), the tripods show the position of the docking points. Two yellow lines, that eventually meet, show the path of those points during approach. It can be seen that the target is tumbling in this specific simulation. Additionally, the pre-calculated abort trajectories are displayed in magenta. For some of them, the initial starting point seems to be the best choice concerning fuel consumption. While the chaser proceeds further on its approaching trajectory, the algorithm made from a mixture of fuel optimization and safety requirements, chooses the second safe point within this setup on the x-axis, this time in front of the target.

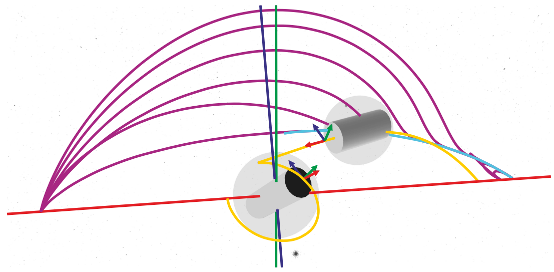

Figure 6. Approach trajectory (cyan) and potential abort trajectories (magenta). The yellow line marks the path of the two docking points that meet eventually.

3.8.1. Propellant Consumption

The required thrust for a successful approach is displayed in Figure 7. The steps mirror the 50 intervals calculated as the thrust will be given in multiple impulses. The closer the chaser gets, the fewer thrust is induced - the reduction of the relative velocity to a minimum for staying within the berthing box and performing the actual grabbing is required. The consumption each trajectory would

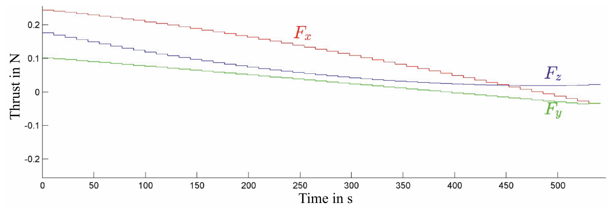

Figure 7. Chronological sequence of the thrust during the approach.

require is displayed in Figure 8. Dependent on the safety requirements (e.g., the safety parameter C_{err}), the value at each point varies. A successful approach takes about 2.67 kg hydrazine, displayed by the vertical line in the figure. Here, eight abort trajectories and the approach trajectory have been calculated e.g., the approach trajectory has been divided into eight, at each point (0/8, 1/8, 2/8, ... 8/8) an abort was derived. With the total maneuver requiring about eight minutes, an abort trajectory is available every 60 sec.

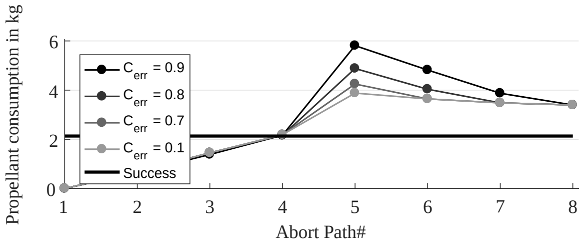

Figure 8. Fuel consumption for different abort trajectories and different safety requirements. The straight line gives the consumption of the approach, the C_{Err} parameters mirror the different safety demands for the abort.

3.9. Considerable future developments

3.9.1. Exchange of Modules

The modules of the simulations will be further specialized. Investigations will concentrate of an improvement of the existing modules and the implementation of missing ones as indicated in Table 1. Especially the failure handling module will be improved in the next steps. Once the simulation fulfills the requirements set, different strategies for a safe approach will be tested as well as different failure scenarios. Those scenarios will include minor failures, which should not lead to an abort, major failures, which should lead in any case to an abort, and failures that have to be classified according to the situation.

Table 1. Overview Modules of the simulation frame

	Simplified	Adjustable
Environment	no perturbations	some effort
Target Body	Cylinder	$\checkmark$
Chaser Body	Cylinder	$\checkmark$
Sloshing	homogenous	some effort
Orbit	Circular	$\checkmark \rightarrow$ Eidel
Optimization	energy	and/or time
Optimizer	OCPID-DAE1	$\checkmark$
Failure implem.	random	some effort

3.9.2. Validation

To proof a newly developed tool, it needs to be validated against existing models. In case of the presented simulation, a transformation into GMAT [16] is momentarily in progress. As the simulation is based on commonly used equations, little deviation is expected. A simple scenario of the approach will be tested to note the deviations. In case both setups processed with the different tools are coherent, it can be assumed, that more complicated ones mirror the environment in the same way.

4. FAILURE SCENARIOS

Further development of the simulation aims to switch between failures that definitely result in an abort, failures that derive from contradictory sensor-data and can be solved without abort and failures, were the momentary capabilities of the chaser decide for or against an abort. Together with an increased autonomy and decision making processes within, failures will be handled according to their level of impact to the system.

Preliminary considerations concerning a failure scenario need to involve the multiple subsystems and according components, the failure would affect. Redundancy of some parts such as the cameras to determine the targets motion are essential. It is assumed, that such failure will be detected and treated with the replacement of the faulty component.
Critical aspects during the approach can either be internal (e.g., a comportment fails) of external (e.g., an obstacle is in the desired flight path). Moreover, a deviation between systematic or mechanical failures can be made. Figure 9 gives the approach to failed power requirements. In this case, the approach is ready to be started, but the system recognizes insufficient power supply and stops the berthing attempt. As this is a symptom, the search for the failed component is essential to overcome the problem.

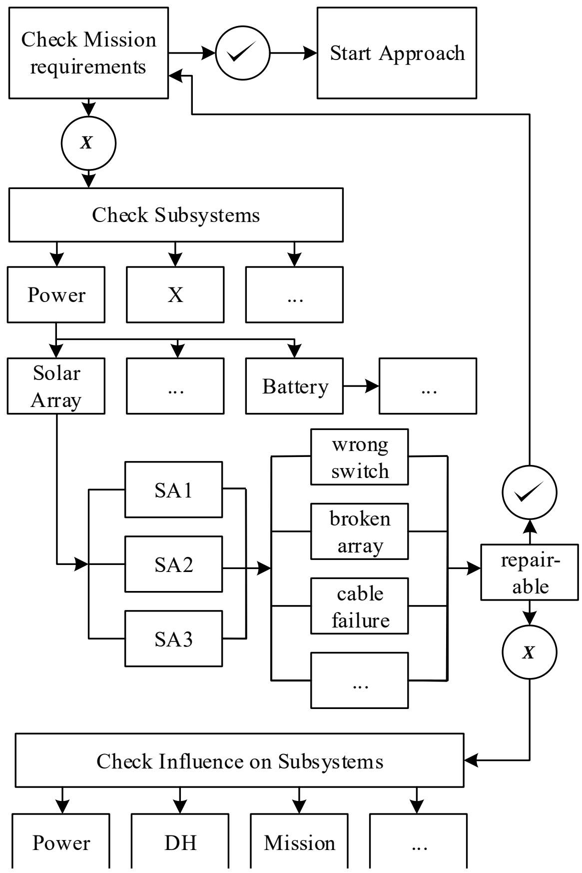

Figure 9. First level of failure scenario approach to determine faulty part and react accordingly.

Finding the failure may not lead to a solution of the problem. In case the failed part is unable to be replaced by a redundant one, the influence a change of the mission has on the other systems needs to be considered. In the displayed version, the a failed solar array could for example change the mission time line if a decision is made to use the other arrays to cover the loss and thus to extend the recharge time of the batteries. Table 2 gives some examples a failed solar array has on the mission and some subsystems. Further on, the system needs to verify, if the specific requirements of the involved subsystems and components will not be violated by the intended solution of the original failure. An optimization process guided by the autonomy concept shall protect the spacecraft.

Table 2. Failure scenario: solar array fails.

Subsystem	Involved Component	Impact
Power	- Solar array	- other arrays need to cover loss
		- buffer covers loss
	- Battery	- increased recharge time
Data Handling	- OBC	- recalculation to protect other sensors
Mission	- time	- may take longer
	- approach	- extra recharge time
	- alignment	- provide more sunlight for other solar arrays

The displayed approach is a very simplified version of the actual decision process. The more parts are included, the more requirements have to be met. Moreover, those requirements will change over time. The modular setup of the presented simulation tool will allow for changes that address complexity and situation specific constraints.

4.1. Autonomy Concept

Various autonomy concepts have been tested on low level for space application. Wander [17] gives an overview of those concepts, resulting in the idea to find the solution in ground-based applications. Unfortunately the formerly considered COSA system [8] was not developed further, documentation is difficult to find. Therefore, the decision has been made to test the developed system on a lower level with one of the Wanders' presented concepts.
As described within this paper, the autonomy module can be replaced within the simulation. In case, a high level autonomy system is available, testing should include the platform developed.

5. SUMMARY

The paper describes a mission concept for the active removal of SL-8 rocket bodies with the intention to slow down the growth of space debris in low Earth orbit. A simulation environment to test different strategies for the part of close vicinity to the target has been derived. It is described in its momentary detail, including considerations that have been investigated. First results and the visualization are shown in the end.

ACKNOWLEDGMENTS

The presented work is supported by Munich Aerospace and Helmholtz Association. The project *Sicherheit im Orbit*, the guiding theme for this work, is a cooperation between DLR and Universität der Bundeswehr München. Additionally, the authors would like to thank Johannes Michael for his support on the simulation implementation. Acknowledgments also go to the students of the Universität der Bundeswehr München that supported this work with their theses.

REFERENCES

1. McKnight D., (2016), Presentation at the *4th Workshop on Space Debris Modeling and Remediation* in Paris, France
2. Inter-Agency Space Debris Coordination Committee (IADC) - http://www.iadc-online.org (21.10.2016)
3. Liou J.-C., et al., (2012). *Stability of Future LEO Environment*. IADC-12-08
4. Peters S., Fiedler H., and Förstner R., (2015). *ADReS-A: Mission architecture for the removal of SL-8 rocket bodies*. IEEE Aerospace Conference.
5. Peters S., et al., (2016). *Mission Concept and Autonomy Considerations for Active Debris Removal*. Acta Astonautica. ISSN 0094-5765. http://dx.doi.org/10.1016/j.actaastro.2016.10.006.
6. NASA, (2013). www.space-track.org (24.06.2014)
7. Gomez H. and Eissfeller B., *Autonomous Determination of Spin Rate and Rotation Axis of Rocket Bodies based on Point Clouds*. AIAA SciTech. http://dx.doi.org/10.2514/6.2016-0886
8. Peters S., et al., (2013). *Research Issues and Challenges in Autonomous Active Space Debris Removal*. IAC-13-A6.5.3
9. Modelict-Konctruktor (2011). http://www.mkonline.ru/2000-07/2000-07-14.html (12.10.2016)
10. Cowardin H., et al. (2011). *Optical Signature Analysis of Tumbling Rocket Bodies via Laboratory Measurements*. AMOS 2012
11. Eidel W., (2015). Bahnanalyse fr Ellipsenbahnen mit $e << 1$. Internal document.

12. Alfriend K., et al., (2009). *Spacecraft Formation Flying: Dynamics, Control, and Navigation*. Elsevier Astrodynamics Series. Elsevier Science.

13. Michael J., et al., (2013). *Optimal Path Planning to an uncontrolled Tumbling Target*. 19th IFAC Symposium on Automation Control in Aerospace

14. Gerdts M. (2010). Optimal Control and Parameter identification with Differential-Algebraic Equations of Index 1. http://www.unibw.de/lrt1/gerdts/software/ocpiddae1.pdf

15. Leuthner J. (2014). Vergleich der Entwicklungen von Erdcomputern mit On-Board-Computern auf Satelliten. Thesis at Universität der Bundeswehr München.

16. NASA - Stephen Hughes. GMAT - General Mission Analysis Tool. https://gmat.gsfc.nasa.gov/. Opensource software.

17. Wander A., and Förstner R., (2012). *Innovative Fault Detection, Isolation and Recovery Strategies on-board Spacecraft: State of the Art and Research Challenges*. DLRK2012-281268